Experimental study of Portevin-Le Châtelier plastic instabilities by infrared pyrometry – Type A to type B transition

Danièle Wagner, Nicolas Ranc

Experimental study of Portevin-Le Châtelier plastic instabilities by infrared pyrometry – Type A to type B transition

D. Wagner[1], N. Ranc[2]
[1]*LEME, University Paris Ouest Nanterre-La Défense, 92410 Ville d'Avray, France*
[2]*LMSP Arts et Métiers Paris Tech,75013 Paris, France*

1. Introduction

In general, at the macroscopic scale the plastic strain in materials is homogeneous. However, under certain conditions of temperature and strain rate, it can become heterogeneous. There is then localization of the plastic strain. The dynamic strain aging (DSA) phenomenon which occurs in some material under certain temperature and strain rate can cause a localization of the plastic strain in the form of bands called bands of Portevin Le Chatelier (PLC). For a tensile test at imposed strain rate, they are associated on the tensile curve with repeated serrations resulting from a succession of stress drops. In the case of test at imposed stress rate, the PLC bands are characterized by discontinuities in the form of levels of strain. This localization of the plastic strain can appear in materials with different crystal lattice (mild steels, austenitic stainless steels, aluminium alloys, zirconium alloys…).
At the macroscopic scale, this phenomenon [1-9], induces an increase in flow stress, ultimate tensile strengh and work hardening coefficient, as well as a decrease in ductility (elongation, reduction of area and fracture toughness) which can be detrimental.
At the microscopic scale, this phenomenon is explained by the dynamic interaction of mobile dislocations with the solute atoms in insertion or substitution. Mac Cormick [3] showed that the slip of dislocations is not continuous, but discontinuous. Dislocations are stopped temporarily on the obstacles (forest, precipitates…) during a waiting time t_w. During this waiting time, an additional anchoring of dislocations by the diffusion of the solute atoms occurs.
The serrations on the stress strain curve obtained at imposed strain rate can be classified in three types according to the spatiotemporal appearance of these bands ([2,4,10-14]). The type C corresponds to the chaotic formation of the bands (discontinuous and not correlated). Each stress drop on the tensile curve corresponds to the formation of one band. The type B corresponds to the discontinuous but regular formation of the bands (each new band is created just above the previous one and so on). Each created band is characterized by a stress drop on the stress strain curve too. Type A bands correspond to a continuous propagation of a band from one edge of the specimen to the other. With each type of band (A, B or C) is associated a type of serration on the stress strain curve, more or less easily identifiable. The occurrence of these different types of bands which correspond to various spatiotemporal types of localization depends on external parameters (level of strain, strain rate, temperature, stiffness of the tensile machine, geometry and surface quality of the samples) and internal parameters (alloy composition, crystal lattice, microstructure and solute atoms type and content, density of mobile dislocations, type of obstacles (forest, precipitates…), grain size of alloy). The

influence of the external parameters (strain rate and temperature) was studied the most in literature. When the strain rate increases (the waiting time of dislocations decreases) or the temperature decreases (mobility of the diffusing species decreases) the localization of the bands evolves from the type C to the type B then type A. Today, the transitions between these various types of bands are not still clearly explained, and the phenomenon modelling is difficult and supplementary knowledge is needed in the mechanism of DSA.
In order to study the spatiotemporal evolution of PLC bands, various authors used the optical extensometry technique (Ziegenbein et al. in 2000 [15], Casarotto et al. in 2003 [16], Klose et al. in 2003 [17], Casarotto et al. in 2005 [18], the technique of speckle interferometry (Shabadi et al. in 2004 [19]), the technique of digital image correlation from a speckle pattern in order to obtain the strain field (Jiang et al. in 2005 [20]). The acquisition frequency of these different devices is about few tens of Hertz. In 2005, Tong et al. [21] and more recently, Ait-Amokhtar et al. [22] used an ultra high speed camera and a technique of digital image correlation to determine the strain field during the formation of a PLC band. This technique allows to visualize very precisely the band formation. Since few years, various authors have developed infra-red thermography technique in order to study PLC bands [23-25]. Indeed the plastic strain is accompanied by a dissipation of the mechanical work in heat what causes generally an increase in the temperature. This technique seems very promising because enables to have a high acquisition frequency during the tensile test (until 400Hz in [24]).
The objective of this paper is more precisely to study with infrared pyrometry technique the influence of the strain and the strain rate on PLC type bands. Within this framework we were interested in an aluminium-copper alloy which enables us to have the PLC phenomenon at ambient temperature. In a first part the experimental device and the analysis method used in this study will be described. In a second part, the results obtained for the type A, type B and type C bands will be presented. Then the evolution of the bands parameters according to strain and strain rate will be detailed and the type A – type B transition will be more particularly discussed.

2. Materials and experimental device

2.1.Materials

The material used in this study is an aluminium-copper alloy EN AW 2024 (4% copper) heat treated at 500°C during 30 minutes and then water quenched. Immediately after quench, the copper concentration content in substitutional solid solution is high and this alloy is sensitive to DSA in a temperature range around 20°C.

2.2. Mechanical tests

Immediately after quench, tensile tests were carried out on a screw driven machine at the ambient temperature. Prismatic specimens of 12mm wide, 3mm thickness and 60mm length were machined. The specimen’s surface was in the as-rolled condition. In order to study the influence of the strain rate on

PLC phenomenon, five tests were carried out at various imposed strain rate ranging between 2.38 x 10^{-4} s^{-1} and 2.14 x 10^{-2} s^{-1} (table 1).

Test reference	Refresh frequency	Type of bands observed	Strain rate in s^{-1}
(1)	25Hz and 500Hz	Type C	2.38 x 10^{-4}
(2)	320Hz	Type A et Type B	4.76 x 10^{-3}
(3)	320Hz	Type A et Type B	1.19 x 10^{-2}
(4)	320Hz	Type A et Type B	2.14 x 10^{-2}

Table 1 : Tests conditions

2.3 Temperature measurement

The measurement of the temperature field on the specimen surface is carried out with a pyrometry technique. Thus an infra-red camera (CEDIP type Jade) whose spectral range is between 3.9µm and 4.5µm is used. The power radiated by the surface of the specimen is collected by an optical system made up of a 50mm focal length objective which is focused on the matrix of the camera. The spatial resolution is of 0.3mm by pixel. An aperture time of the camera of 1500µs allows to detect temperatures ranging between 5°C and 50°C. The noise of the camera is around 20mK. Except in the case of test 1, the refresh frequency of the camera is of 320Hz what corresponds to a period of 3.125 ms. For data storage reasons during the long tests, the refresh frequency during test 1 is reduced to 25Hz or improved to 500Hz in order to have a greater precision in a part of the test. The pyrometer is calibrated on a black body in order to obtain the relation between the signal delivered by the camera and the temperature of the observed surface. In order to neglect the effect of the surface emissivity on the determination of the temperature, all the specimens are covered with a fine coat of black paint.

3. **Results and discussion**

3.1. Macroscopic appearence of the bands

3.1.1. Observation of type A bands

For the tests (2), (3), (4) and for weak nominal strain, a continuous propagation of a plastic strain front (type A band) occurs. The figure 1a shows the temperature evolution versus time in a point B located at the center of the specimen. A sudden increase in the temperature is measured when the plastic strain front crosses on the point B. For the test (2) at a nominal deformation of 3.9% (figure 1a), the temperature increment is estimated at 0.18°C. The figure 1b shows three thermographies when the band crosses on the measurement points A, B and C defined on the figure 1a. The increment of temperature is calculated with the initial temperature field at the time t_0 = 7.409s corresponding to the beginning of the band propagation on the right-hand side of the specimen.

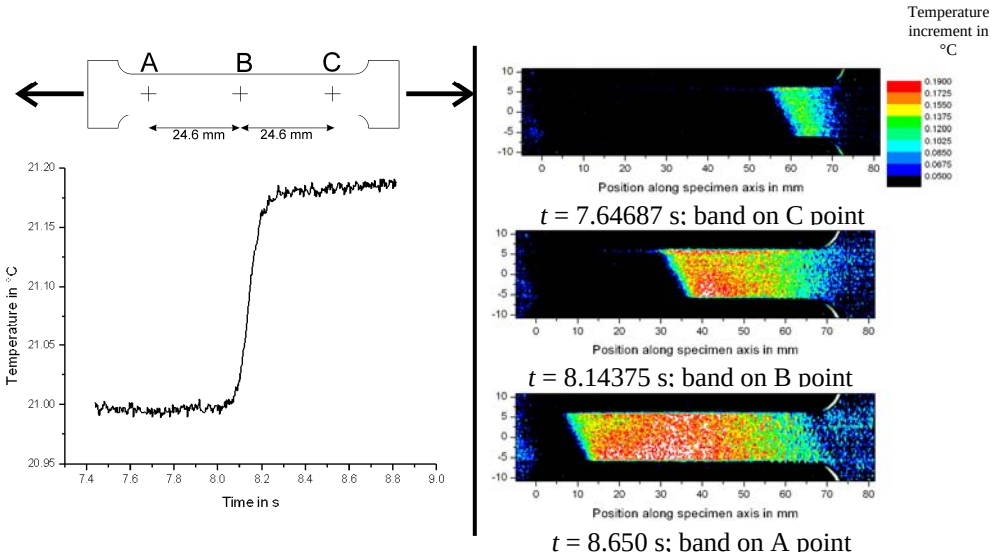

a) b)

Fig. 1. Test (2) at a nominal strain ε = 3.88% a) temperature evolution in the center of the specimen during the type A band propagation, b) fields of temperature increment.

These three thermographies allow to determine the slope angle of the propagation front with the axis of the specimen and to measure the propagation velocity of this plastic strain front. In the case of the test (2) and for a nominal strain of 3.9% we find an angle of 63±1° and a propagation velocity of 49.5 mms^{-1} between the points C and B and 48.6 mms^{-1} between the points B and A.

3.1.2. Observation of type B bands

For the tests (2), (3) and (4) at higher strains, we can notice the presence of a discontinuous propagation of type B bands. They are characterized on the stress strain curve (figure 2) first by regular small serrations (a) of increasing amplitude during the test and second by more significant serrations (b). Each small serrations correspond to the formation of one PLC band and the stronger serrations correspond to the formation of several PLC bands at the extremity of the specimen. This aspect was detailed in [23]. Figure 2 shows the conventional stress-strain curve and the temperature measured on three points of the sample noted A, B and C and spaced of 24.5 mm (figure 1a). The temperature recordings at the A, B, C points (figure 2) show a sudden increase of the temperature when a band goes in front of the measurement point.
Figure 3 shows the evolution of the temperature in the center of two consecutive bands according to the time. We can notice an increase in the temperature which corresponds to the plastic strain during each band formation. In the case of the test (3) (figure 3), for a nominal strain of 15.8%, the temperature increment during the formation of the first band (t = 13.291s) is 0.74°C. This curve allows to define the time of band formation and the time between two consecutive bands noted respectively t_f and t_{mb}. The time of band formation is defined as the time corresponding to the temperature increase from 5% to 95% of the total temperature increment in the band (see figure 3). In the case of the test (3), for a nominal strain of 15.8%, the time of band

formation can be estimated at 7.8ms for the first band and 6.3ms for the second. Figure 3 also allows to define the time between two consecutive band formations. We suppose that the moment of band formation is the time when the increase in temperature in the band reaches 50% of the total temperature increment. In the case of figure 3, time between two band formations is about 51.7ms for a nominal strain of 15.8%.

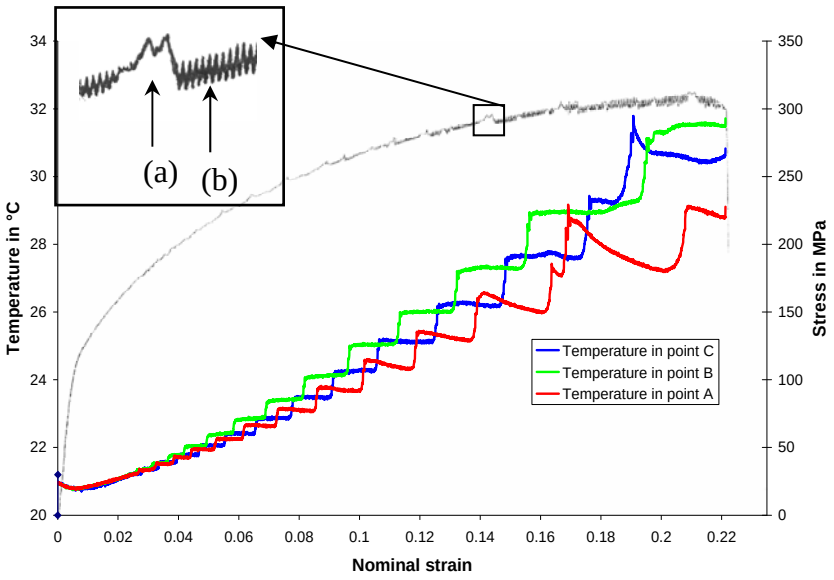

Fig 2. Stress-strain curve and temperature evolution for test 3

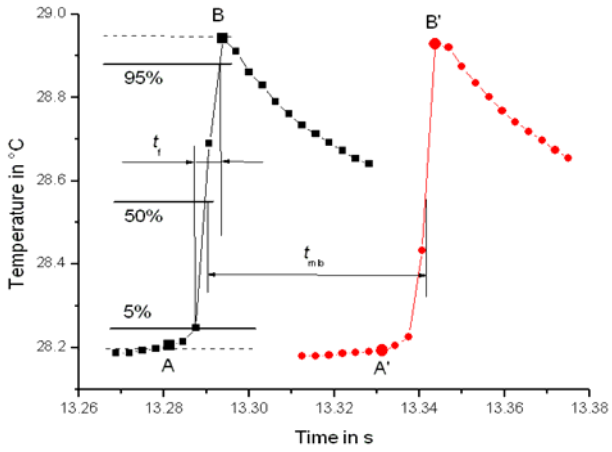

Fig. 3. Temperature evolution in the center of two consecutive bands during test (3) (strain rate : 1.19 x 10^{-2} s^{-1})

From thermographies of temperature increment, other geometric characteristics can be measured (see details in [25]). The slope angle between the band direction and the specimen traction axis is of 61±1°. In the case of the test (3) and for a nominal plastic deformation of 15.81%, the bandwidth along the traction axis noted *d* and the distance between two consecutive bands

noted δ are respectively equal to 2.9±0.15 mm and 1.4±0.15 mm. This bandwith is measured from temperature measurement along the specimen axis.

3.1.3. Observation of type C bands

For lower strain rate (for example 2.38 x 10^{-4} s^{-1} for the test (1)), the stress strain curve does not present any more significant serrations corresponding to the formation of bands on the edges of the specimen as in the case of type B. Regular stress jumps are then observed whose amplitude is more significant than in the case of type B bands and increases during the test [25]. These serrations are always associated with the formation of PLC bands but those are formed in a random way along the specimen (type C bands). For a nominal strain of 13.7%, we can measure a time between two bands of 3.7s and a slope angle of the band with the specimen axis of 58±1°. In order to measure with sufficient precision the duration of band formation, we carried out a thermal recording at a frequency of 500Hz. Then, we find for a nominal strain of 13.7% and a strain rate of 2.38 x 10^{-4} s^{-1} a duration of band formation of 3.7ms. The temperature increment in the band is of 1.04°C and the bandwidth is of 3.7±0.15 mm.

3.2. Evolution of the characteristics of the bands according to the nominal strain and strain rate

Taking into account the precision of our experimental device, we did not measure significant variation of the slope angle of the bands between the 3 types. However, we highlighted a slight increase in the bandwidth from type B to type C (table 2).

Test reference	Strain rate in s^{-1}	Observed type band	Slope band	Bandwith
(2) at ε = 3.88%	4.76 x 10^{-3}	A	63±1°	----
(3) at ε = 15.8%	1.19 x 10^{-2}	B	61±1°	2.9±0.15 mm
(1) at ε = 13.7%	2.38 x 10^{-4}	C	58±1°	3.7±0.15 mm

Table 2. Slope band and bandwidth measurements from type A to type B

On the other hand, it is more interesting to measure the time between two band formations t_{mb} (figure 4)(case of type B and type C), the time of band formation t_f (figure 5) (case of type B and type C), the apparent propagation velocity (figure 6) (type A, type B) and the increment of plastic deformation in a band (figure 7)(type A, type B and type C) (for details, see [25]).
Figure 4 shows the evolution of the time between two band formations according to the nominal strain for four strain rates when this quantity is measurable. It is noted that time between two band formations increases with the nominal strain and decreases when the strain rate increases. The increase of the time between two band formations with the nominal strain was already noted by Jiang et al. [20] in an Al4%Cu alloy. More recently Ait-Amokhtar et al. [22] also showed in experiments that this time between two bands (called reloading time) increases when the nominal strain increases. This effect can be explained by the fact that the waiting time of mobile dislocations and thus

the time between two band formations increase with the strain. Indeed, we can express the waiting time t_w according to elementary plastic deformation noted Ω and the strain rate: $t_w = \Omega / \dot{\varepsilon}$. It can be consider that the elementary plastic deformation increases linearly with the strain [26]. An increase in the nominal strain thus results in an increase in the waiting time and thus an increase in the time between two band formations. The relation also allows to explain the increase in the waiting time and thus in the time between two band formations with a decrease in the strain rate. For the type C (obtained for low strain rate or high temperature) the diffusion of solute atoms is enhanced, the anchoring of mobile dislocations increases and so the time between two bands (so the waiting time t_w) increases and is greater than in type B.

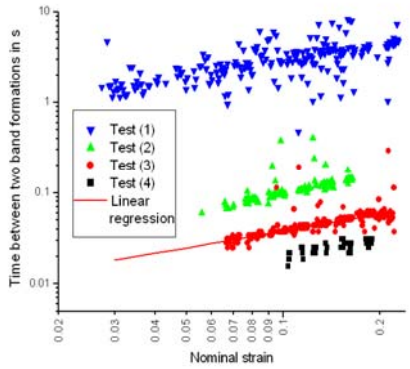

Figure 4. Evolution of t_{mb}

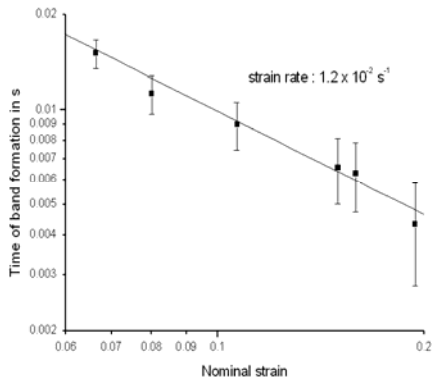

Figure 5. Evolution of t_f

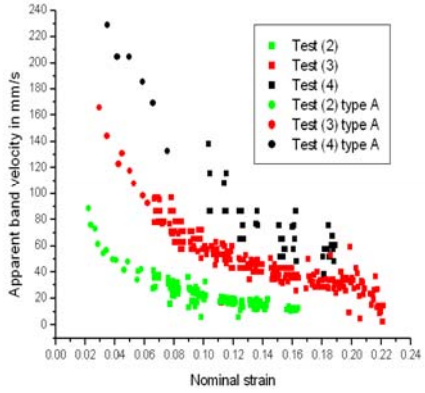

Figure 6. Evolution of band velocity

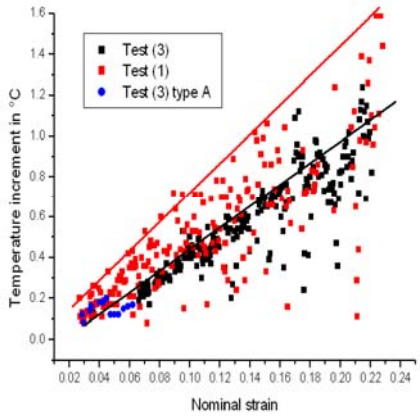

Figure 7. Temperature increment in the band

The evolution of the band formation time (figure 5) has been measured for test (3) in the case of type B band. For the type C, this time of band formation has been measured from the test performed at low strain rate with a camera frequency of 500Hz. For ε =13.7%, we find a duration of band formation of 3.7ms. The values which we find in this study are the same order as those measured by Louche et al [24] (the development time of the band is estimated at 10 ms in an alloy Al-4wt.%Mg) and by Tong et al. [21](the development

time of the band is estimated between 3ms and 5ms in an alloy Al-2.5wt.%Mg). However no data is available in the literature concerning the evolution of this time of band formation according to the nominal strain. For type C, the time for the band formation is smaller than in type B.
The band spacing (measured for type B only and not reported here, for more details see [25]) is constant or decreases weakly with the strain. No effect of the strain rate can be detected.
Figure 6 represents the apparent propagation velocity according to the nominal strain. As the distance between two band remains constant or decreases weakly when the strain increases and the time between two band formations increases when the strain increases, a decreasing apparent speed is well noted when the strain increases. An increase in the apparent propagation velocity with the strain rate of the test can also be highlighted. If we put on figure 6, the values of propagation velocities of the plastic strain front in the case of the bands of type A, we can observe a continuity between this front velocity and the apparent propagation velocity of the type B bands.
Figure 7 shows the temperature increment associated with each band according to the nominal strain and the strain rate.

3.3. Type A – type B transition

During the test (3), a transition from type A bands towards type B bands appears when the nominal strain increases. The value of the nominal strain when the transition occurs is difficult to evaluate, because in a strain range around this transition we show at the same time bands of type A and bands of type B. Also it is easier to define the strain range of the transition. We can estimate this transition strain range between 5% and 6%.
In order to explain this transition from type A to type B, we are more particularly interested in the comparison between time of band formation and time between two band formations. Fig. 4 shows the evolution of the time between two band formations (t_{mb}) according to the nominal strain when this quantity is measurable. It is noted that time between two band formations increases with the nominal strain. On Fig. 4, we can show that the evolution of the time between two band formations follows a linear law with the nominal strain in a log-log diagram. Thus, we can write a relation between t_{mb} and the nominal strain ε:

$$t_{mb} = A\varepsilon^{B} \quad \text{with} \quad A = 0.15\text{s} \ \text{et} \ B = 0.6068 \quad \text{(for test (3))} \quad (1)$$

The standard deviation between the experimental results and the regression is of 0.07s. Fig. 6 shows the evolution of the time of band formation (t_f) according to the nominal strain in the case of the bands of type B. The curve on Fig. 6 highlights a reduction in the time of band formation with the strain. In a log-log diagram, this evolution can be considered as linear. A linear regression enables us to obtain a power law evolution of the time of band formation according to the strain:

$$t_f = F\varepsilon^{G} \qquad \text{with } F = 0.0008\text{s} \qquad \text{and} \qquad G = -1.0925 \qquad (2)$$

On the Fig. 8, the time between two bands formations t_{mb} and the time of band formation t_f are plotted versus ε from equations (1) and (2). For one strain, the two straight lines intersect. On the left hand of the intersection, the time of band formation t_f is greater than the time between two bands formations t_{mb} . In this case, it is impossible to distinguish two consecutive band formations and we are in a continuous propagation of the plastic strain front that is to say in type A band. From Fig. 8, the intersection is for the same order of deformation that the experimental value (5–6%) determined for the transition type A-type B for the test performed for this study.

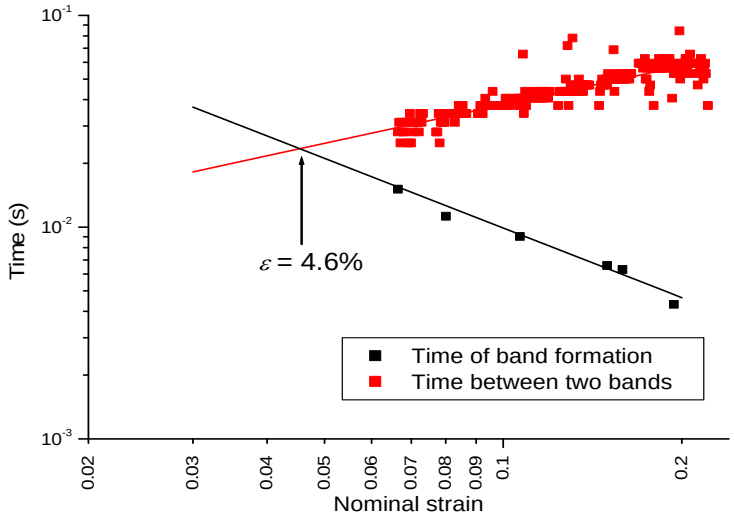

Figure 8. Comparison between t_{mb} and t_f

4. Conclusion

In this paper, we studied the Portevin Chatelier bands of type A, B and C in a Aluminium Copper alloy using the temperature measurement technique of infra-red thermography. We are more particularly interested in the study of the band characteristics such as the distance between two consecutive bands, the time of band formation, the time between two band formations, the bandwidth, the slope angle with the axis of the specimen and the temperature increment in the bands. We also studied the evolution of these various characteristics according to the nominal strain and the strain rate. In particular, we highlighted an increase in the time between two band formations and a reduction in the time of formation with an increase in the nominal strain. We noted that in the case of bands of type B which corresponds to a discontinuous propagation, the time of band formation is lower than the time between two band formations. We also showed that the type A – type B transition from a continuous propagation towards a discontinuous propagation corresponds to the equality between the time of band formation and the time between two band formations.

References :

[1] J.D. Baird, Dynamic Strain Aging in : The Inhomogeneity of Plastic Deformation, 191; 1973, Ohio, ASM Metals Park.
[2] L. J. Cuddy, WC. Leslie, Some aspects of serrated yielding in substitutional solid solutions of iron, Acta Metall.Mater., 20 (1972), 1157-1167.
[3] P.G. McCormick, A model for the Portevin-Le Chatelier effect in substitutional alloys, Acta Metall., 20 (1972), 351-354.
[4] J. L. Strudel, Interactions des dislocations avec les impuretés mobiles in Dislocations et déformation plastique, (ed. P. Groh, L.P. Kubin, J.L. Martin) (1979) Paris, Les éditions de la physique, 199-222.
[5] H. Neuhäuser, C. Schwink in : Cahn RW, Haasen P, Kramer (Eds), Vol. 6. (1993) London, Materials Science and Technology.
[6] Y. Estrin, LP. Kubin, in H.B. Mühlhaus (Eds),in : Continuum Models for Materials with Microstructure (1995), New York,Wiley, 395-450.
[7] D. Wagner, JC. Moreno, C. Prioul, Rev. Met., 12 (2000),1481-1500.
[8] D. Wagner, JC. Moreno, C. Prioul, J.M. Frund, B. Houssin, Rev. Met., 5 (2001) 473-483.
[9] D. Wagner , JC. Moreno, C. Prioul, J.M. Frund, B. Houssin, Jl of Nuclear Materials, 300 (2002) 178-191.
[10] B.J. Brindley, P.J. Worthington, Yield point phenomena in substitutional alloys, Metall. Rev. 15 (1970) 101-114.
[11] P. Lacombe, L'effet Portevin – Le Chatelier, ses caractéristiques et ses conséquences sur les hétérogénéités de déformation plastique, Matériaux et Techniques, 1985, E5 –E15.
[12] P. Rodriguez, Strain Aging, Dynamic, in: R.W. Cahn (Ed.), Encyclopedia of Materials Science and Engineering, Supp vol.1, Pergamon, 1988, pp. 504-508.
[13] P.G. McCormick, S. Venkadesan, C.P. Ling, Propagative instabilities : an experimental view, Scripta Metall. Mater. 29 (1993) 1159-1164.
[14] M. Lebyodkin, L. Dunin-Barkowskii, Y. Bréchet, Y. Estrin, L. P. Kubin, Spatio-temporal dynamics of Portevin-Le chatelier effect : experiment and modelling, Acta Mater. 48 (2000) 2529-2541.
[15] A. Ziegenbein, P. Hähner, H. Neuhäuser, Comput. Mater. Sci., Correlation of temporal instabilities and spatial localization during Portevin-LeChatelier deformation of Cu-10%Al and Cu-15%Al, 19 (2000) 27-34.
[16] L. Casarotto, R. Tutsch, R. Ritter, J. Weidenmüller, A. Ziegenbein, F. Klose, H. Neuhäuser, Comput. Mater. Sci., Insvestigation of PLC bands with optical techniques, 26 (2003) 210–218.
[17] F.B. Klose, A. Ziegenbein, J. Weidenmüller, H. Neuhäuser, P. Hähner, Portevin-LeChatelier effect in strain and stress controlled tests, Comput. Mater. Sci. 26 (2003) 80-86.
[18] L. Casarotto, R. Tutsch, R. Ritter, H. Dierke, F. Klose, H. Neuhäuser, Comput. Mater. Sci. 32 (2005) 316–322.
[19] R. Shabadi, S. Kumar, H.J. Roven, E.S. Dwarakadasa, Mater. Sci. Eng., Characterisation of PLC bands using laser speckle technique, A364 (2004) 140-150.
[20] Z. Jiang, Q. Zhang, H. Jiang, Z. Chen, X. Wu, Mater. Sci. Eng. A403 (2005) 154–164.
[21] W. Tong, H. Tao, N. Zhang, L.G. Hector Jr., Scripta Mater, Time-resolved strain mapping measurements of individual Portevin-LeChatelier deformation, bands 53 (2005) 87–92.
[22] H. Ait-Amokhtar, S. Boudrahem, C. Fressengeas, Scripta Mater. 54 (2006) 2113–2118.
[23] N. Ranc, D. Wagner, Mater. Sci. Eng. A394 (2005) 87-95.
[24] H. Louche, P. Vacher, R. Arrieux, Mater. Sci. Eng. A404 (2005) 188–196.
[25] N. Ranc, D. Wagner, Mater. Sci. Eng. A474 (2008) 188–196
[26] M. Zaiser, P. Hähner, Mater. Sci. Eng. A238 (1997) 399–406.